Mon. Not. R. Astron. Soc. **265**, 588–600 (1993)

The opacity mechanism in B-type stars – II. Excitation of high-order *g*-modes in main-sequence stars

W. A. Dziembowski,[1] P. Moskalik[1] and A. A. Pamyatnykh[1,2]
[1] *Copernicus Astronomical Center, ul. Bartycka 18, 00-716 Warszawa, Poland*
[2] *Institute of Astronomy, Pyatnitskaya 48, Moscow 109017, Russia*

Accepted 1993 May 25. Received 1993 May 25; in original form 1993 January 28

ABSTRACT

We show that the OPAL opacities, in addition to explaining the origin of the pulsations of β Cep stars, also predict the existence of a large region in the main-sequence band at lower luminosities, where high-order *g*-modes of low harmonic degree l are unstable. The excitation mechanism remains the same, and is due to the usual κ-effect acting in the metal opacity bump ($T \approx 2 \times 10^5$ K). The new instability domain nearly bridges the gap in spectral types between δ Sct and β Cep stars. The periods of the unstable modes are in the range 0.4–3.5 d for $l = 1$ and 2. We propose that this excitation mechanism causes photometric variability in the slowly pulsating B-type stars (SPB stars), and perhaps in other B stars for which variability in the same period range has been reported.

Typically, a large number of modes are simultaneously unstable in one model. Most of them have $l > 2$. Such modes are not likely to be detected photometrically, but may be visible in line profile changes. The excitation of many high-l modes in a star may also cause a spurious contribution to the rotational $v \sin i$ values.

Sequences of unstable modes at each value of l exhibit a periodically varying departure from equal spacing in period. This feature, first noted in white dwarf *g*-mode spectra (calculated and measured), is in the present case a probe of the region left behind the shrinking core (the μ-gradient zone). We discuss prospects for and difficulties of SPB-star asteroseismology.

Key words: instabilities – radiative transfer – stars: early-type – stars: interiors – stars: oscillations.

1 INTRODUCTION

The pulsational instability of stars located on the main sequence between the β Cep and δ Sct instability strips has been suspected for many years. The first suggestion came from Struve (1955), who proposed that a new class of variables, oscillating with periods of 0.1–0.3 d, might exist between spectral types B7 and A2. He named these stars the Maia variables, after the prototype. Struve later abandoned the idea, but other observers continued the search for such stars (see McNamara 1987b for a summary). The results have been negative, and in no object has a short-period variability been conclusively proven. Interestingly, however, McNamara (1985, 1987a) has found a *long-period* photometric variability in three Pleiades stars: Merope (B6IVe), Atlas (B8III) and Pleione (B8Vpe). The detected periods are between 0.5 and 3.8 d, which is well above the range proposed by Struve for the Maia stars. Such long periods, if real, and if associated with pulsations, must correspond to the high-order non-radial *g*-modes.

Towards the end of the 1970s, Smith & Karp (1976) and Smith (1977) discovered periodic or quasi-periodic changes in the line profiles of 53 Per and a few other slowly rotating stars. These changes have been interpreted as resulting from non-radial oscillations with low spherical harmonic degrees, l (Smith 1977). With the single exception of 10 Lac, all the 53 Per-type stars fall between the spectral types of B0 and B5, and about two-thirds of them are located on the Hertzsprung–Russell (HR) diagram either on the lower edge or below the β Cep domain. This is the case, for example, for ι Her (B3IV) and for 53 Per itself (B4IV). The observed periods are typically in the range of 0.5–2.0 d. The periods, though, are rather difficult to determine from the sparse spectroscopic data, and therefore they very often differ from one observing run to another. Some of the 53 Per-type stars have been also found to vary photometrically. In the best-studied case, of 53 Per, Smith et al. (1984) have determined two stable periods of 1.68 and 2.16 d. Even for this object, however, the exact value(s) of the period(s) or even the very reality of the multiperiodic behaviour remains a matter of controversy (Balona 1987; Le Contel et al. 1989). Such a situation has prompted Balona (1987) to suggest that explanations of the 53 Per phenomenon other than non-radial pulsations might be possible.

The breakthrough in the search for pulsations in B-type main-sequence stars came with the series of excellent photometric papers by Waelkens. First, Waelkens & Rufener (1985) analysed a large body of data collected in the Geneva system, concluding that a higher than average variability occurs for the intermediate B-type stars. In a number of objects, which have been monitored over a long period of time, coherent periodic brightness variations have been found, with a semi-amplitude of several mmag and a period of between 1 and 3 d. In all cases, colour variations have also been observed, and they have been in phase with the variations of brightness. In a subsequent paper, Waelkens (1991) has shown that all these stars are in fact *multiperiodic*, with up to eight independent frequencies simultaneously present in one star. This finding proves that the variability is caused by pulsations. The length of the periods and the phase relation between the light and colour curves clearly point towards pulsations in the high-order *g*-modes.

Thanks to the large quantity and high homogeneity of data, Waelkens's (1991) work has unambiguously established the existence of a new class of variable stars: the slowly pulsating B-type (or SPB) stars. His original sample of variables consisted of only seven objects. Four additional members of the group have recently been identified (210 G. Eri: Manfroid & Renson 1989; HD 34798 and 45284: Heynderickx 1991; HD 37151: North, private communication to Grenon 1992), as well as several likely candidates (Burki 1983; van Genderen et al. 1992; Jerzykiewicz & Sterken 1992; see also Waelkens & Rufener 1985, table 2). All these stars are main-sequence objects, their spectral types range from B3 to B8 [with the exception of two variables from Jerzykiewicz & Sterken (1992), which have types of B1III and B2III], and they all share the same pulsational properties. The spectral types and periods of 53 Per and ι Her also fall in the pertinent range, which suggests that they might belong to the SPB class as well. Such a link between the SPB and the 53 Per-type variables has been already proposed by Waelkens & Rufener (1985), and has been further supported by the discovery of line profile changes in two SPB stars: o Vel and HD 74560 (Waelkens 1987). We also note that both of these groups of variables are slow rotators, even though the SPB stars have been selected on purely photometric grounds. Finally, the three Pleiades variables identified by McNamara can also be related to the SPB group, although the values of $v \sin i$ for these objects are rather high (see table 1 of McNamara 1987a). Thus the emerging observational picture indicates that small-amplitude, long-period pulsations occur in main-sequence B-type stars quite often. It is now the turn of theory to understand what causes these stars to vary.

In Paper I (Dziembowski & Pamyatnykh 1993; see also Moskalik & Dziembowski 1992), we demonstrated that oscillation modes observed in β Cep stars are indeed unstable in the corresponding stellar models built with the new OPAL opacities (Iglesias, Rogers & Wilson 1992). The driving is due to the κ-mechanism acting in the metal opacity bump at temperatures of $T \approx 2 \times 10^5$ K, which is a new feature not present in the earlier opacity data. In addition, we found an instability to high-order *g*-modes with much longer periods (above 0.8 d). This instability appears only for spherical harmonics of relatively high degree, $l \geq 6$. Thus excitation of such modes is not likely to lead to a photometric variability. We pointed out, however, that in models of less luminous stars the instability range should shift towards lower l-values and still longer periods, and we proposed that this instability is responsible for the variability of the SPB stars.

In this paper, we report results of a stability survey of the main-sequence stellar models in the mass range of 2.5–7.0 $M_\odot$. In Section 2 we describe the methodology of the calculation. The physics of the driving effect is described in Section 3, while the properties of *all* unstable modes in a selected model are reviewed in Section 4. We also speculate in Section 4 about the possible finite-amplitude consequences of the instability. Next, in Section 5, we present the theoretical domains of instability in the HR and period versus log $T_{\rm eff}$ diagrams, and we compare them with observational data. The extensive stability survey leading to the determination of the domains was carried out by considering only modes with $l \leq 2$. A potential significance of the SPB stars for asteroseismology is discussed in Section 6.

2 THE METHOD

We used the same stellar evolution and stellar oscillation codes as in Paper I. Thus we shall outline here only the most important aspects of the calculation, especially those that are relevant for an understanding of the difference between our conclusions and those of Degryse et al. (1992). These latter authors conducted a similar stability survey and concluded that the long-period modes in the SPB stars are excited primarily by the κ-mechanism operating in the He II ionization zone. As we shall discuss shortly, this result is not supported by our calculations.

We used the newest version of the OPAL opacity tables (Iglesias et al. 1992). Two-dimensional (in logarithms of the table arguments) cubic spline formulae were adopted for the log κ interpolation, and the opacity derivatives needed in the oscillation code were calculated analytically (see Mosakalik & Dziembowski 1992). In evolving models, special care was taken to secure a smooth behaviour of the Brunt–Väisälä frequency in the chemically inhomogeneous zone left behind the shrinking core. The treatment of convection was standard. We allowed no convective overshooting from the core, and in the envelope we used the mixing-length formalism. We adopted one pressure distance-scale for the mixing length in our calculation. As expected, the role of convective transport in the envelopes of the models considered was found to be very small. The diffusion approximation for the radiative flux was assumed to be valid throughout the whole star, including the atmosphere. Models were calculated assuming an initial hydrogen abundance of $X = 0.7$ and a metallicity parameter $Z = 0.02$ (main survey) or $Z = 0.01$.

Oscillations were treated as fully non-adiabatic in the outer layers. The quasi-adiabatic approximation was adopted automatically in the interior whenever it was formally justified (Dziembowski 1977a). In the convective regions we neglected the Lagrangian perturbation of the convective flux and we ignored the eddy viscosity. These crude approximations are probably inconsequential in the case of oscillations of B-type stars, because the role of convective regions in determining the mode stability is always very small. The same applies to our crude treatment of the atmospheres. The oscillation code introduces additional zoning, which depends on the behaviour of eigenfunctions. For the high-order *g*-modes considered in the present work, up to 6000 mesh points were needed to secure the target accuracy of 10^{-4} in the calculated frequencies.

3 THE EXCITATION MECHANISM

A mode excitation due to the opacity mechanism may occur only if certain requirements concerning the shape of the eigenfunction, as well as the ratio of oscillation period P to thermal time-scale $\tau_{\rm th}$ in the potential driving zone, are satisfied. More precisely, the first requirement is that the pressure eigenfunction $\delta p/p$, where δ is the Lagrangian perturbation, is possibly large and varies slowly with r within the driving zone. We have seen in Paper I (fig. 8) that in the β Cep stars we encounter the shape that is favourable for the driving in the lowest order (both *p*- and *g*-) modes and then again in quite high-order ($n \sim 20$) *g*-modes. The pressure eigenfunction for the latter modes has the outermost maximum in the driving zone. The value at this maximum is much larger than at the local maxima located deeper in the star.

The second requirement is that $\tau_{\rm th}/P$ must not be much less than 1. Otherwise, the potential driving layer remains in thermal equilibrium during pulsations and therefore is neutral. In models of β Cep stars, the metal opacity bump is located in a relatively shallow layer where $\tau_{\rm th}$ is well below 1 d. For the high-order *g*-modes, the time-scale constraint is then fulfilled at $l \geq 6$. With decreasing l, we have to increase the period of the modes in proportion to $[l(l+1)]^{-1/2}$, in order to maintain the same favourable shape of the eigenfunctions. The time-scale requirement is then no longer satisfied. This is why we do not find instability to high-order *g*-modes of *low* degrees l in the β Cep models (Paper I). In the less-massive models the bump is located in deeper layers and, in addition, the luminosity is lower. Both factors contribute to an increase of $\tau_{\rm th}$ at the metal opacity bump, and consequently the low-degree *g*-modes can now be driven.

In Fig. 1 we show two models, which are representative of the SPB and the β Cep stars, respectively. The plots demonstrate that the driving mechanism in both cases is essentially the same. All quantities are plotted as functions of temperature in the models. In this way, all important features in opacity occur at nearly the same positions. The He II ionization bump is located at $\log T \approx 4.6$ and the metal opacity bump is at $\log T \approx 5.3$. The value of the Rosseland mean opacity, κ, is systematically larger in the 4-M$_\odot$ model, which reflects its larger densities. More important for the driving is the opacity derivative. In this case only subtle differences between the two models are visible. The thermal time-scale plotted in the third panel is defined as

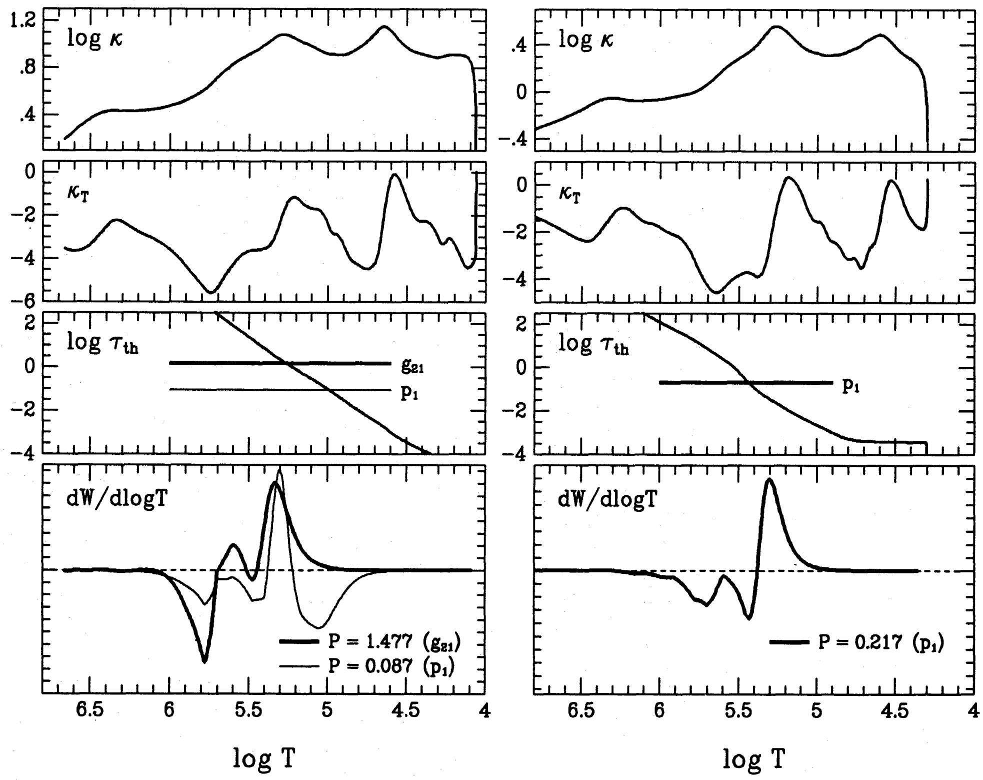

Figure 1. Opacity κ, opacity derivative $\kappa_T = (\partial \ln \kappa / \partial \ln T)_\rho$, thermal time-scale $\tau_{\rm th}$ (see equation 1) and differential work integral $dW/d \log T$ (arbitrary units, positive in driving zones), for selected pulsation modes, plotted versus temperature. Left-hand panel: SPB-star model [$M = 4$ M$_\odot$, $\log(L/{\rm L}_\odot) = 2.51$, $\log T_{\rm eff} = 4.142$, $X_c = 0.37$]; right-hand panel: β Cep-star model ($M = 12$ M$_\odot$, $\log(L/{\rm L}_\odot) = 4.27$, $\log T_{\rm eff} = 4.378$, $X_c = 0.13$). Both models have an initial composition of $X = 0.7$ and $Z = 0.02$.

$$\tau_{\rm th}(T)=\frac{\int_0^{M(T)} c_P\,\mathrm{d}M}{L}, \tag{1}$$

where $M(T)$ denotes the mass calculated from the surface downward to the point with temperature T. One may see that $\tau_{\rm th}$ in the vicinity of the metal opacity bump is about 1.5 orders of magnitude larger in the SPB model than in the β Cep model. This explains the preference for excitation of long-period modes in lower luminosity stars. The plots of contributions to the work integral, W, for the g_{21}-mode and the p_1-mode in the models of the SPB and the β Cep stars, respectively, exhibit a remarkable similarity. In both cases, the contribution to W from the deeper layers ($r<0.46R$ and $r<0.40R$, respectively) is negligible.

The plot of $\mathrm{d}W/\mathrm{d}\log T$ for the p_1-mode in the SPB model explains why acoustic modes are not excited at lower stellar luminosities. For such short-period modes, the damping layer located between the metal bump and the He II ionization bump becomes activated. A large negative contribution to W arising in this layer causes an overall mode stability. From the similar time-scale argument alone, one could expect to find an instability of very high-order p-modes driven by the He II bump. This instability does not occur, because for such modes the eigenfunctions are changing too rapidly with r. For the same reason, acoustic modes of $n>2$ in the β Cep star models are stable (Paper I), despite the fact that their periods match $\tau_{\rm th}$ at the metal opacity bump better than do the periods of modes with $n=0$–1.

In contrast to the conclusions of Degryse et al. (1992), we did not find any noticeable contribution to g-mode excitation from the He II ionization zone in any of the models; neither did we find any significant ε-mechanism contribution from the core. Regarding the role of the He II layer, the use of the quasi-adiabatic approximation by Degryse and her collaborators is the primary suspect, as in fact was noted already by the authors. We have performed a test quasi-adiabatic calculation for the case in which the reported driving effect in the He II zone is the largest, and we have also found an instability. Clearly, this is an artefact of an unjustified use of the quasi-adiabatic approximation in layers where $\tau_{\rm th}\ll P$. It is more difficult to understand the second difference. In all main-sequence models that we considered, there was a positive contribution to W from the convective core, but it was always several orders of magnitude less than that from the envelope driving layers. An inadequate spatial resolution of the models used by Degryse et al. is the only explanation that comes to mind.

The only important driving effect that we see in our survey is that of the metal opacity bump. This effect could not be found by Degryse et al. (1992), because they used the Los Alamos opacity data in which this bump is not present.

4 UNSTABLE MODES

In this section we focus on a single model of 4 $\mathrm{M}_\odot$ in the middle of the main-sequence band. This is the same model as used in Fig. 1, and it may be regarded as representative of the whole class.

4.1 Growth rates and other linear properties

As a measure of mode instability it is useful to consider, along with the ordinary growth rate γ, a normalized growth rate η, defined by Stellingwerf (1978), as follows:

$$\eta=\frac{W}{\int_0^1\left|\frac{\mathrm{d}W}{\mathrm{d}r}\right|\mathrm{d}r}. \tag{2}$$

While $\gamma=-\mathrm{Im}(\omega)$, where ω is the complex eigenfrequency, is a measure of the time-scale connected with the mode excitation or damping, η is a measure of dominance of driving over damping effects within the star. Thus the latter determines the robustness of the instability, and perhaps gives a better estimate of the chance that the mode will survive in the finite-amplitude development of the instability.

Both growth rates are plotted in Fig. 2. In the upper plot the values of γ as a function of P are given for all unstable modes in the model. At $l=1$ the instability begins with the radial order $n=14$. This initial value of n increases with l, and for consecutive l-values it is 15, 15, 17, 17, 21 and 22. The total number of unstable modes, taking into account $2l+1$ values of the azimuthal number m, is 1344. Variations of γ with l and P reflect variations not only of W, but also of the mode inertia. The latter are responsible for relatively low γ-values in the $l=1$ sequence, and for the structure in the $\gamma(P)$-dependence. Values of η provided in the lower plot are

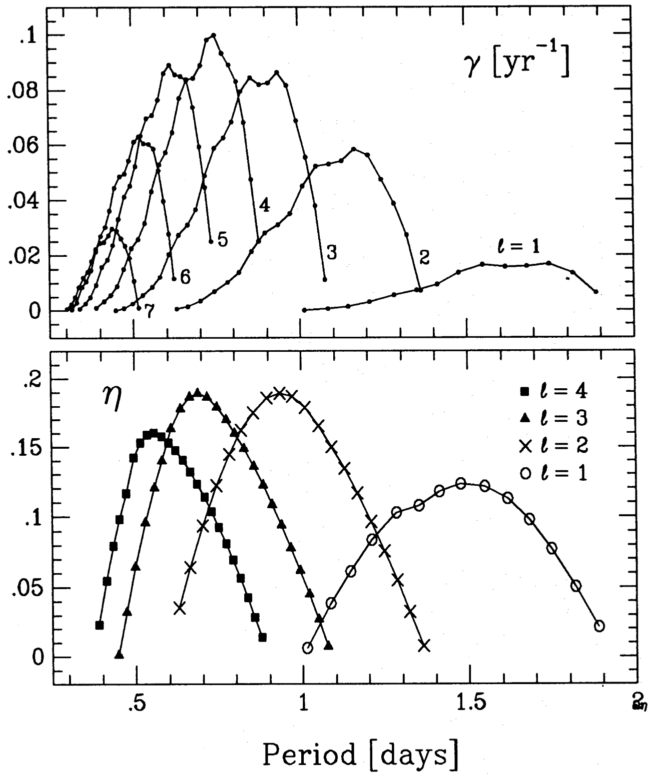

Figure 2. Values of growth rate γ and normalized growth rate η (see equation 2), versus period for unstable modes with different l-values in the SPB model of Fig. 1. There are no unstable modes for $l\geq 8$.

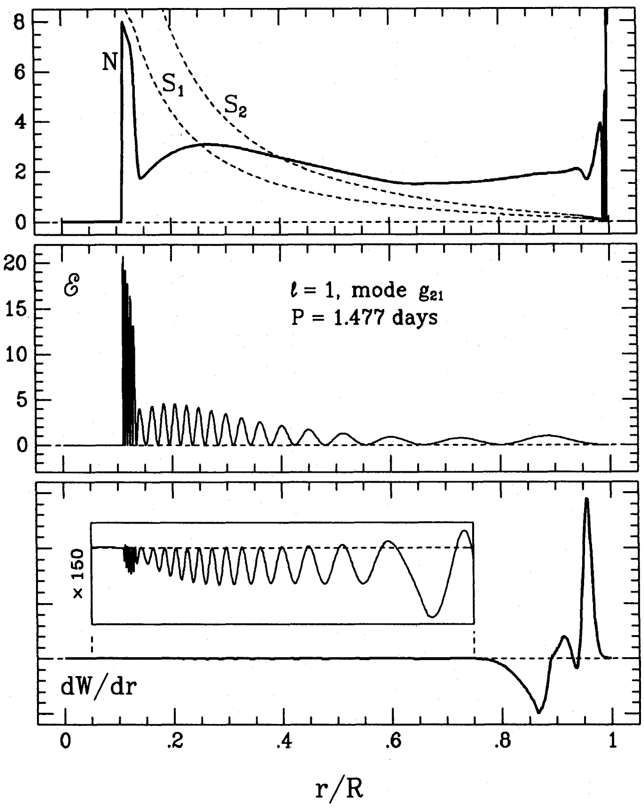

Figure 3. Top: critical frequencies in the SPB model of Fig. 1. N is the dimensionless Brunt–Väisälä frequency and the S_l are Lamb frequencies (the p_1, $l=0$ mode has a frequency of $\sigma \approx 2$ in these units, and a period of 1 d corresponds to $\sigma = 0.185$). Middle: kinetic energy density for the most unstable $l=1$ mode in the model. The normalization $\int_0^1 \mathscr{E}\, \mathrm{d}x = 1$ is adopted. Bottom: differential work integral, $\mathrm{d}W/\mathrm{d}r$ (arbitrary units), for the same mode.

quite large. The maximum values, reaching nearly 0.2, are larger than the corresponding values in the δ Sct and β Cep models (Dziembowski 1993), and are comparable to those encountered in the classical Cepheids.

The unstable modes are indeed of high order, and some of their properties may be understood with the help of the asymptotic theory thoroughly discussed in the context of white dwarf oscillations (see e.g. Kawaler 1990). One may see in Fig. 2 that the separation between consecutive modes at fixed l is nearly constant in period. We will return to the question of mode spacing in Section 6.

In Fig. 3 the behaviour of the critical frequencies in the selected SPB model is shown. The frequencies are given in units of $\sqrt{4\pi G\langle\rho\rangle}$. In this model the dimensionless frequency is related to the oscillation period P (in days) by $\sigma = 0.185/P$. The well-known conditions for the gravity-wave propagation are

$$\sigma < N \qquad \text{and} \qquad \sigma < S_l.$$

We may see that they are satisfied in almost all of the radiative interior. The sharp rise of N at $r/R = 0.15$ corresponds to the mass point located at the convective core boundary at the beginning of the main-sequence evolution of the star. Downwards from that point to the current boundary of the convective zone ($N=0$), the radial gradient of the mean molecular weight is responsible for large values of N.

The contributions from various layers to the kinetic energy density and to the total work integral of a selected mode are shown in the same plot. One should note that almost all of the contribution to W arises in the outermost wave. One may also see that, even with the 150× magnification, the contribution from the ε-mechanism cannot be distinguished. In more evolved models, the role of the μ-gradient zone is much more important. In fact, a sharp increase of dissipation in this zone is responsible for the termination of the instability, shortly before the end of the main-sequence phase of evolution.

Finally, let us note that the layers contributing to W are stable against convection ($N>0$). This is true in almost all models relevant to the SPB stars. Only in the coolest models in the 7-$M_\odot$ sequence does a thin convective zone develop. This zone grows with the stellar mass, but even in the β Cep models convection remains inefficient. In the present case there is only a dip in N at $r \approx 0.95$. This is a pleasing aspect of the models considered in this paper, because the treatment of convection is always the least reliable part of the linear stability calculations.

4.2 Amplitudes

The theoretical evaluation of unstable mode amplitudes lies in the domain of non-linear theory. The theory, however, has not yet been developed to a level that enables a prediction of the finite-amplitude outcome of a multimodal instability, such as is encountered in the present case. What can be done within the framework of the linear theory is an evaluation of the amplitudes for various observables, assuming some arbitrary normalization of the eigenfunctions. In order to put some physics into the normalization, we have considered non-linear saturation of the driving mechanism as the cause of amplitude limitation.

For the driving effect, the behaviour of opacity or of its derivatives is critical. We may therefore expect that the feedback effect of multimodal excitation on the mean model will be large when it causes an appreciable change of any of these quantities. Let f be the opacity or its derivative (for this qualitative argument it does not matter which), and for simplicity assume that f depends only on temperature. Thus its mean change due to the oscillations is given by

$$f(T) - f(T_0) = \frac{1}{2}\frac{\partial^2 \ln f}{\partial \ln T^2} \sum_{k=1}^{K} \left\langle \left| \frac{\delta T}{T} \right|^2 \right\rangle_k, \qquad (3)$$

where $\langle\rangle$ denotes averaging over the surface and K is the total number of excited modes. It is clear that the contribution from the linear term is averaged out. In Fig. 4 we plot the $\delta T/T$ amplitude in the outer part of the model for three selected $l=1$ modes. For all three modes, the same surface value of $\delta T/T$ has been arbitrarily adopted. For the saturation effect, the relevant amplitude is that in the driving region. Thus, to calculate the observables, we normalized $\delta T/T$ in the region where $\mathrm{d}W/\mathrm{d}r$ is large. Specifically, for every mode (when excited alone), we adopted

$$\left\langle \left| \frac{\delta T}{T} \right|^2 \right\rangle_k = 0.1 \qquad \text{at} \qquad r = 0.96R. \qquad (4)$$

Because the coefficient of the sum in equation (3) is of the order of unity or more, this normalization means that every excited mode exerts a significant feedback effect on the model. If there are K excited modes and each of them makes the same contribution to the saturation then the calculated amplitudes should be divided by $\sqrt{K}$.

The amplitudes plotted in Fig. 5 were evaluated using a simple formalism developed by one of us (Dziembowski 1977b), based on the Eddington atmospheric model. There have been subsequent improvements in the method, consisting of the use of more realistic models, but for our purpose it was not necessary to employ these more laborious methods. The rapid decrease of the observable amplitude with l is caused by the effect of averaging contributions of opposite sign over the stellar disc. The increase of $A_{\rm mbol}$ with P may be easily understood with the help of Fig. 4. Let us first note that, in these high-order g-modes, $A_{\rm mbol}$ is dominated by the relative variations of the effective temperature. One may see that the latter grows with period if $|\delta T/T|$ is kept constant in the driving layer. Thus in photometric observations we are strongly biased towards detecting modes of low l-values and long periods. In radial velocity measurements, the first trend is weakened and the second is reversed.

If all 1344 unstable modes were excited to similar amplitudes in the driving layer then the amplitudes plotted in Fig. 5 would have to be divided by a factor of ~ 37 ($\sqrt{1344}$). This would imply that the best visible modes have ~0.01-mag amplitudes, which is somewhat lower than the typical values for the SPB stars (Waelkens 1991). We know, however, that such a scenario cannot be true, because excitation of that many high-l g-modes would result in spectral line broadening significantly larger than the $v \sin i$ values measured in SPB stars (which are 5–40 km s^{-1}: Waelkens 1987). With the adopted normalization, we found that the line broadening due to oscillation would be of the order of 100 km s^{-1}. This number only weakly depends on $\sin i$ and mode composition. The implication of little line broadening in the SPB stars could be that either the saturation of the driving mechanism takes place at much smaller amplitudes that we have assumed, or the amplitude limitation occurs through a different mechanism, e.g. resonant mode coupling (see e.g. Dziembowski 1992).

5 DOMAINS OF LOW-DEGREE MODE INSTABILITY

We have limited our survey to models of $l \leq 2$ because our main goal is to explain the photometric variability of B-type stars. The inclusion of higher l-values would lead to an upward extension of the high-order g-mode instability domain in the HR diagram. We have shown in Paper I that at $l \geq 6$ this instability is still present in a sequence of 12-M$_\odot$ models.

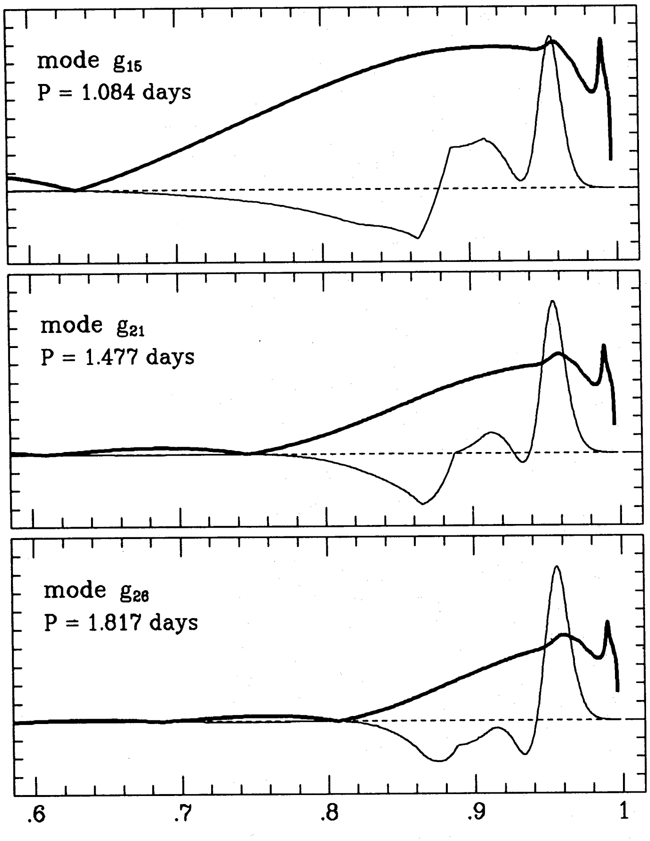

Figure 4. Relative temperature perturbation $\delta T/T$ (thick lines) and differential work integral $\mathrm{d}W/\mathrm{d}r$ (thin lines), for selected unstable modes of the SPB model of Fig. 1.

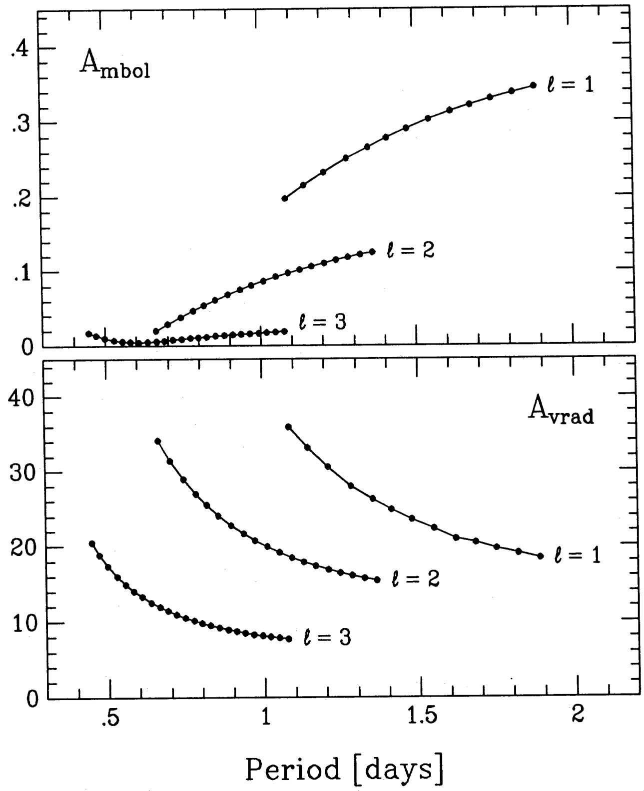

Figure 5. Amplitudes of bolometric brightness variations (in mag) and radial velocity variations (in km s^{-1}) for unstable g-modes of $l \leq 3$ in the SPB model of Fig. 1. The normalization given by equation (4) is adopted. The expected amplitudes depend on inclination angle i through the factor $P_l^m(\cos i)$. The amplitudes plotted are rms values averaged over solid angles.

5.1 Three instability domains in the main-sequence band

In Fig. 6 we compare the position in the HR diagram of the high-order g-mode instability domain with the positions of domains corresponding to the δ Sct and β Cep stars. For the δ Sct domain we plot only the blue edge. The position of the red edge cannot be determined in a reliable way because it depends on the interaction between oscillations and convection, which is not well understood. The blue edge of the δ Sct domain was determined for $l=0$ modes, but it is essentially the same as for other low-l modes. On the zero-age main sequence (ZAMS) the instability starts at p_8. With the luminosity increase, the instability of the highest order modes gradually disappears.

The δ Sct domain is regarded as a low-luminosity extension of the Cepheid instability strip. This is justified, because the driving mechanism remains almost unchanged in spite of the large difference in luminosity. The dominant role is played by the He II ionization zone, and low-order p-modes are unstable. The two remaining domains owe their existence to the instability driven by the metal opacity bump. There is, however, a discontinuous change in the nature of the unstable modes between these two domains. It is interesting that, in the mass range extending from 1.5 to 17 $M_\odot$, there is

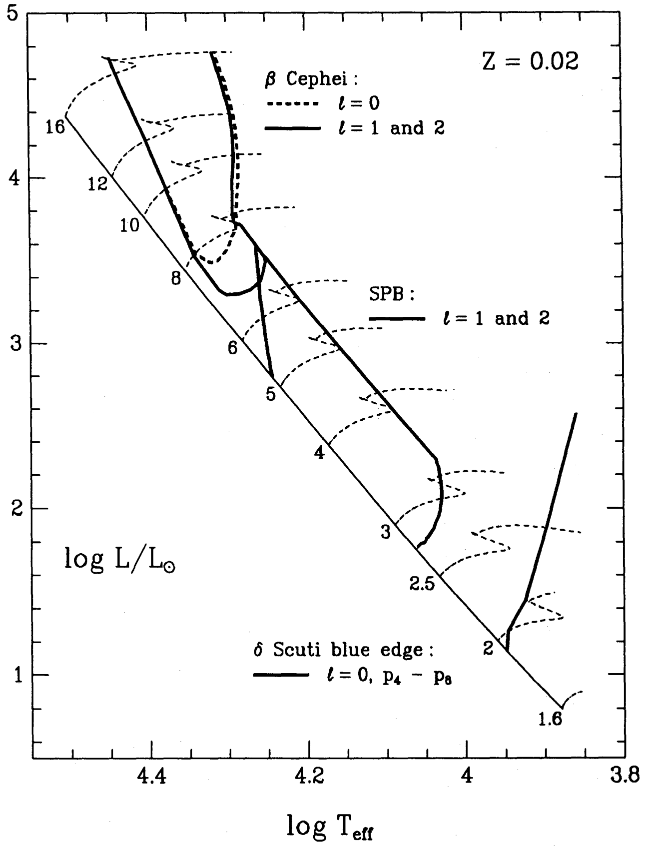

Figure 6. Regions of the HR diagram where the opacity mechanism causes instability of low-degree modes. Each region may be associated with a specific type of variable star. The values of l are spherical harmonic degrees of the modes included in the stability survey. Thus $l=1$ and 2 means that at least one mode of either of the two degrees is unstable within the region boundaries. Some of the evolutionary tracks used in the survey are shown.

only a narrow gap at about 2.5 $M_\odot$ where main-sequence stars avoid an instability driven by the κ-mechanism. In terms of spectral types, the stability gap covers A0–A1.

The β Cep instability strip was plotted on the basis of the survey presented in Paper I. We plotted the boundary for $l=0$ and that for the $l=1$ and 2 modes separately. In the lower part of the strip, only g-modes are unstable. These are the low-order modes, whose properties in the driving region are quite similar to those of the low-order p-modes. It is therefore justifiable to regard this domain as a part of the β Cep instability strip. The possibility that g-modes may be excited in a β Cep star has been suggested by Waelkens & Heynderickx (1989).

We use the name *SPB domain* to denote the part of the main-sequence band where the instability to the high-order g-modes occurs. The instability disappears before the end of hydrogen burning in the core. The cause, as pointed out in Section 4.1, is an increasing dissipation in the deepest radiative layers, which once were part of the convective core. In terms of position in the HR diagram, the end of instability occurs shortly after the minimum of $T_{\rm eff}$ in the main-sequence phase. Let us recall that hydrogen burning in the core ends at the subsequent $T_{\rm eff}$ maximum. In principle, the situation is different from that in the β Cep domain. There, the instability of radial and of some non-radial modes survives well past the end of the core burning phase. The end of the instability in the evolutionary track is determined by non-adiabatic effects occurring only in the outer layers. The large difference in the speed of evolution between the main-sequence and post-main-sequence phases, however, allows us to regard the locus of the minimum temperature in the main-sequence phase as an effective red boundary of the β Cep strip as well.

5.2 Comparison with observations

We shall try to demonstrate in this section that the κ-mechanism acting in the metal opacity bump is responsible for the observed g-mode pulsations in the SPB stars, and that the variability observed in some other B-type stars may have the same origin. The argument will be based on the coincidence of the variable stars with the instability domains in the HR and P versus log $T_{\rm eff}$ diagrams.

Let us consider first the relevant part of the HR diagram. In Fig. 7 we show the instability domains for $l=1$ and $l=2$ spherical harmonics separately. One may see that all the SPB stars (asterisks) lie within the theoretical instability strip. The positions of HD 37151 and 45284 cannot be regarded as a problem, because the calibration of $\log(L/L_\odot)$ may be uncertain by more than 0.2. For example, the Strömgren photometry (Hauck & Mermilliod 1990; with the calibrations of Balona & Shobbrook 1984 and Balona 1984) yields, for HD 37151, $\log(L/L_\odot)=2.21$, which places the star in the middle of the main-sequence band. The position of the three Pleiades stars of McNamara (1987a) may be regarded as being within the instability domain as well. Because Waelkens & Rufener (1985) have suggested that the SPB and the 53 Per-type stars might belong to the same class of variables, we have also marked in Fig. 7 ι Her and 53 Per itself. These two objects are among the coolest 53 Per-type stars in the sample by Smith & Karp (1976). As we see, they are both placed well within the theoretical SPB strip.

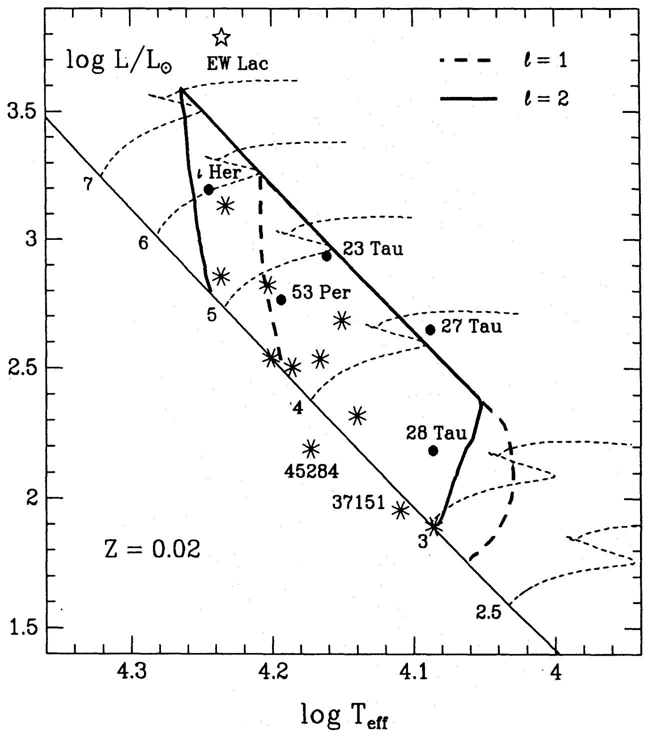

Figure 7. Domains of high-order *g*-mode instability in the HR diagram, compared with positions of observed SPB stars (asterisks) and some other slowly variable B-type stars (dots). $T_{\rm eff}$ and L for SPB stars are taken from Heynderickx (1991), except for HD 27563 and 37151. For these two stars, and for 53 Per and ι Her, parameters are derived by authors from Geneva photometry (Rufener 1988; with the calibration of North & Nicolet 1990) in the same manner as in Heynderickx (1991). For three Pleiades stars, parameters are taken from Grillo et al. (1992), and for EW Lac parameters come from Floquet et al. (1992).

The periods of the unstable modes in the five studied sequences of stellar models are shown versus the effective temperature in Fig. 8. The periods range from 0.4 d up to about 3.5 d. The largest values are achieved for 4- and 5-$M_\odot$ models, which are located in the middle of the theoretical SPB domain. In Fig. 9 a comparison with observational data is shown. In most cases the observed periods fall within the theoretically predicted range, and thus may be associated with unstable *g*-modes of low *l*. The plot also shows that we cannot account for the excitation of some of the longest period modes, notably in HD 74195 and 27563. The discrepancy is not big enough to shake our belief in the identification of the driving mechanism, but demands explanation in future works. The positions of the Pleiades stars in Fig. 9 suggest that they should be included in the SPB class. The same is also true for 53 Per. Two additional periods reported for this star by Balona & Engelbrecht (1985) (0.8613 and 0.6798 d) fall into the theoretical SPB domain as well. The location of 53 Per in Figs 7 and 9 supports the conjecture of Waelkens & Rufener (1985) that 53 Per-type variables and the SPB stars might be closely related.

5.3 High-order *g*-modes and periodic variability in Be stars

The region of the HR diagram where the SPB variables occur is also populated by the Be stars, which between spectral types of B0 and B7 constitute about one-fifth of all main-sequence objects (e.g. Slettebak 1988). A large subgroup of the Be stars, sometimes referred to as the λ Eri-type variables, display periodic photometric variability with periods of between 0.4 and 3.0 d (Balona 1990). In many of these stars, the low-order line profile variations are also seen. These observations are usually interpreted either in terms of non-radial pulsations (Baade 1988) or in terms of a rotational modulation (Balona 1991). Because the multiperiodicity has not yet been convincingly proven for any of the λ Eri variables, both hypotheses are still viable as an explanation of the phenomenon.

It is interesting to note that the spectral range of the Be stars largely overlaps the theoretical domain of the high-order *g*-mode instability. Also, the periods measured for the λ Eri-type stars are in the same range as those of the unstable *g*-modes. As an example, we have displayed in Figs 7 and 9 the variable EW Lac, for which multiperiodicity of the line profile variations has recently been reported (Floquet et al. 1992). In the HR diagram (Fig. 7) this star falls above the instability strip, but this can be attributed to the uncertainty of $\log(L/L_\odot)$ inferred from Floquet et al., which could be in error by as much as 0.2 (formal 1σ error bar). Thus the star might actually lie within the strip. Also, in the P versus $T_{\rm eff}$ diagram (Fig. 9) the periods of EW Lac are in rough agreement with the theoretically predicted range. Thus it is possible that the same high-order *g*-mode instability that explains the pulsations of the SPB stars might also be the cause of the variability in the λ Eri-type stars. We should also note that in many of the λ Eri variables a residual scatter, sometimes labelled *flickering*, is seen. According to Balona (1990), 'the flickering component (in the power spectra) is very low or absent for frequencies exceeding 5 d^{-1}, and rises to a flat maximum for frequencies lower than 2 d^{-1}'. This behaviour could be a signature of the presence of many unresolved, low-amplitude pulsation modes, which according to the theory should be excited in this period range. We have to issue a reminder here, however, that in the pulsation calculations presented in this paper the effects of rotation have been ignored. In contrast to the SPB case, the Be stars are all very fast rotators, with $v_{\rm rot} \sin i$ reaching 400 km s^{-1}. A direct extension of our results to these objects must therefore be regarded with caution.

5.4 Influence of the metal abundance

We saw in Paper I that the extent of the β Cep instability domain determined for the metal abundance of $Z = 0.03$ is considerably larger than that obtained with the standard value of $Z = 0.02$. For the lower mass stars considered in the present work, the effect is much smaller. Therefore we will not present here any of the results obtained with $Z = 0.03$. Instead, we show in Fig. 10 the instability domain calculated for $Z = 0.01$. We found that, at this low value of the metallicity parameter, the β Cep domain is absent. On the other hand, the SPB domain still has a considerable size. Thus if in a stellar system for an appropriate range of spectral types we do not see the β Cep-type pulsation, but we do see the SPB-type pulsation, we may consider a moderately low metallicity as an explanation.

Balona (1992) has reported results of the CCD photometry of NGC 330, a blue globular cluster in the Small

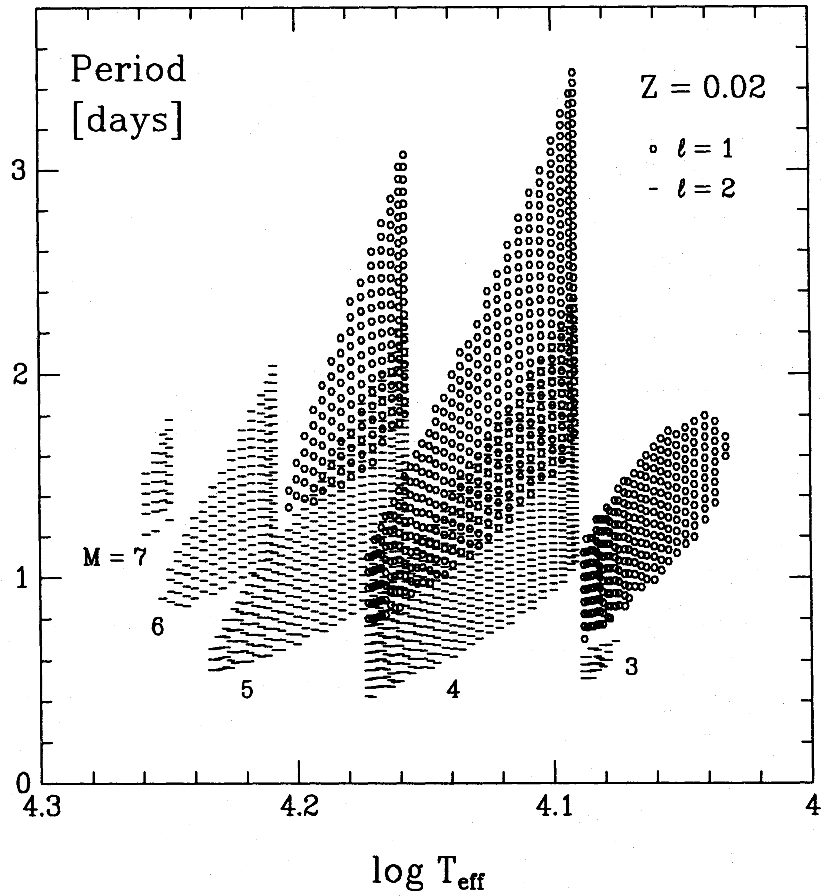

Figure 8. Periods of unstable high-order g-modes in sets of main-sequence modes with $M=3$–$7\ \mathrm{M}_{\odot}$. $l=1$ and $l=2$ modes are shown separately.

Magellanic Cloud. He has discovered a number of λ Eri variables, but found no evidence for the presence of β Cep stars. Based on this finding, he argues that the mechanism causing variability in the former type of star is apparently independent of the metallicity (which is low in the SMC), and thus cannot be the same as in the β Cep case. Our results show that the g-mode oscillations driven by the opacity mechanism must still be regarded as a viable explanation for the variability of λ Eri stars.

6 PROSPECTS FOR ASTEROSEISMOLOGY

In a typical SPB model, a large number of modes with $l \leq 2$ are unstable and can be seen (e.g. Fig. 2). Already, up to eight frequencies have been detected in one star (HD 160124: Waelkens 1991), and additional periodicities are probably present. This richness of the frequency spectrum makes SPB stars particularly promising targets for asteroseismology.

In all models contained in this study, only the models with high radial order n are unstable, and such modes can be accurately described by the asymptotic theory. For a given spherical harmonic degree l, the g-modes with consecutive values of n are asymptotically equidistant in period. The spacing ΔP is given by (Tassoul 1980; see also Kawaler 1990).

$$\Delta P_l = \frac{2\pi^2}{\sqrt{l(l+1)}\int_{r_1}^{r_2} N\,\mathrm{d}\ln r}. \tag{5}$$

The integration of the Brunt–Väisälä frequency N is carried over the whole g-mode propagation zone which, as Fig. 3 shows, is nearly the same for all the modes and extends through almost the whole radiative interior. In Fig. 11 we plot the values of $\Delta P = P_{n+1} - P_n$ as a function of P_n for $l=1$–4 in a representative model of the SPB star. We also show with thin lines the asymptotic values of ΔP_l given by equation (5). As can be seen, the periods are indeed very nearly equally spaced for each l, although small departures from the equidistant pattern are present. The *average* period spacing is predicted by the asymptotic theory very accurately. This confirms the applicability of such a theory to the SPB stars.

An interesting consequence of equation (5) is that the ratio of period spacings for two different l values is a function only of the l-values involved. For example, for modes with $l=1$ and 2 the ratio $\Delta P_{l=1}/\Delta P_{l=2} = \sqrt{3}$. Provided that enough frequencies have been detected, this property can be used for the identification of l-values [see the example for a white dwarf star (Winget et al. 1991)]. The value of ΔP itself also

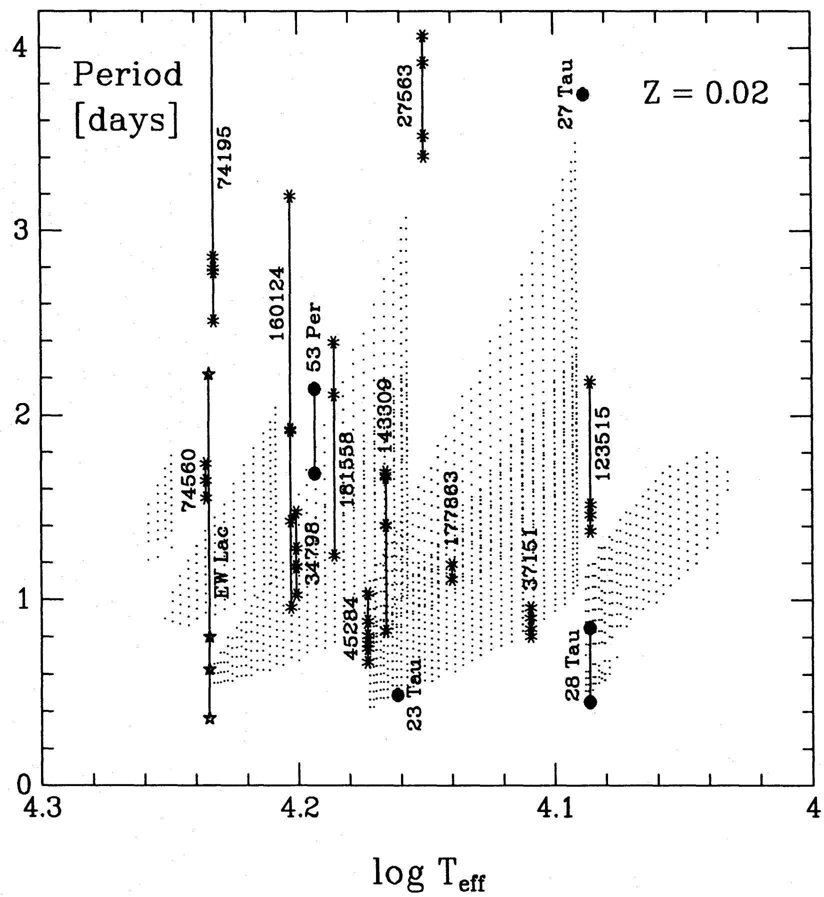

Figure 9. Periods observed in SPB stars (asterisks) and other slowly variable B-type stars (dots), compared with theoretical periods of unstable g-modes (cf. Fig. 8). Observational data are taken from Waelkens (1991), Heynderickx (1991), Manfroid & Renson (1989), North (private communication to Grenon 1993), McNamara (1987a), Smith et al. (1984) and Floquet et al. (1992). T_{eff} is as in Fig. 7. Stars are labelled by name or HD number.

contains important asteroseismological information. In the SPB models this parameter is rather sensitive to the stellar mass and, for a given mass, to the effective temperature. Thus the measurement of ΔP, combined with the measurement T_{eff}, will allow accurate determination of the mass and age of the star.

The deviations from the uniformity of the period spacing ΔP are not random, but display a regular, oscillatory pattern. With increasing l these deviations become smaller, although their *relative* size remains about the same. The periodic behaviour of ΔP is very reminiscent of the behaviour found in the white dwarf models (e.g. Brassard et al. 1992; Bradley, Winget & Wood 1993), as well as in the real white dwarf stars (Winget et al. 1991). In the case of the white dwarfs, the departure from equidistant spacing is caused by the chemical stratification of the envelope, which produces local steep gradients in the Brunt–Väisälä frequency and consequently leads to the 'mode trapping' phenomenon. The trapped modes have most of their energy contained in the surface helium layer. Their periods are also affected and, as a result, their distance in period from the mode of the next *lower n* is smaller than the asymptotic value. With our definition of ΔP, a trapped mode is recognized as the mode immediately *to the right* of the ΔP minimum.

Analysis of the numerical results shows that the periodic pattern of ΔP in the SPB models is also related to the mode trapping. This time, the trapping occurs in the μ-gradient zone on the surface of the convective core, where the Brunt–Väisälä frequency is locally much higher. This is illustrated in Fig. 12, where we show the kinetic energy density for two modes of $l=2$: g_{16} and g_{18}. The former corresponds to the minimum of ΔP. It has a node at $r/R=0.137$ (close to the minimum of N), and consequently it is partially trapped between that point and the point of $r/R=0.110$ (where $N=0$). The g_{18}-mode, shown for comparison, is not trapped and its energy in the μ-gradient zone is much lower. In the ΔP plot, the g_{18}-mode is located near the maximum. We note that, although the mode trapping in the SPB models significantly affects the period spacing, its effect on the *overall energy* of the modes is very small, much smaller than in the white dwarfs. This is why the growth rates γ in our models show only minute variations with the trapping cycle (see Fig. 2). In contrast to the case of the white dwarfs (Winget, van Horn & Hansen 1981), in the SPB stars the trapping cannot act as a mode selection mechanism.

The mode trapping phenomenon can serve as a very sensitive tool to probe the deep interiors of the SPB stars, particularly of their μ-gradient zones. For example, the length of the

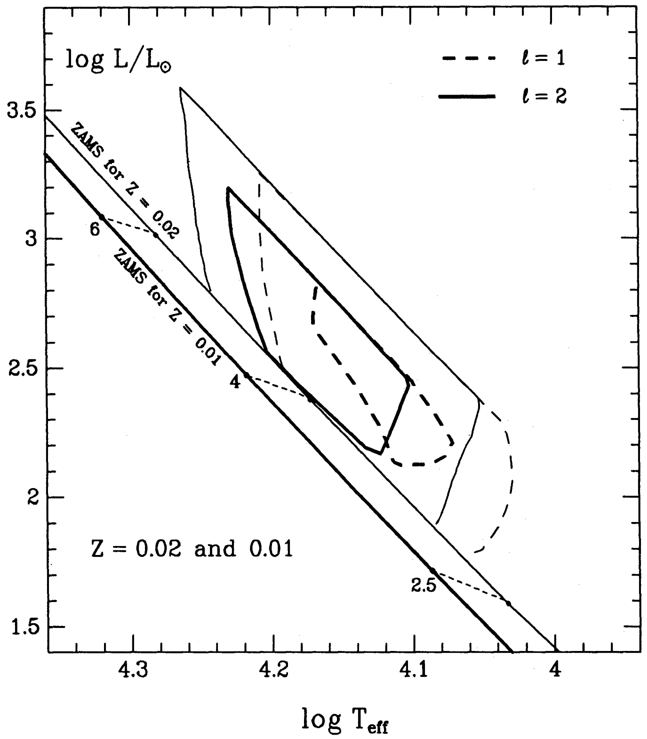

Figure 10. Low-degree g-mode instability domains for two values of the metal abundance parameter Z.

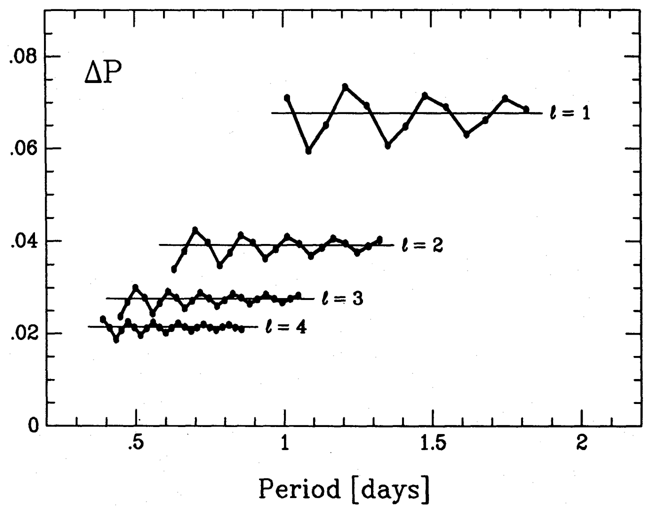

Figure 11. The g-mode period spacing in the SPB model of Fig. 1. Thin lines mark theoretical values given by equation (5).

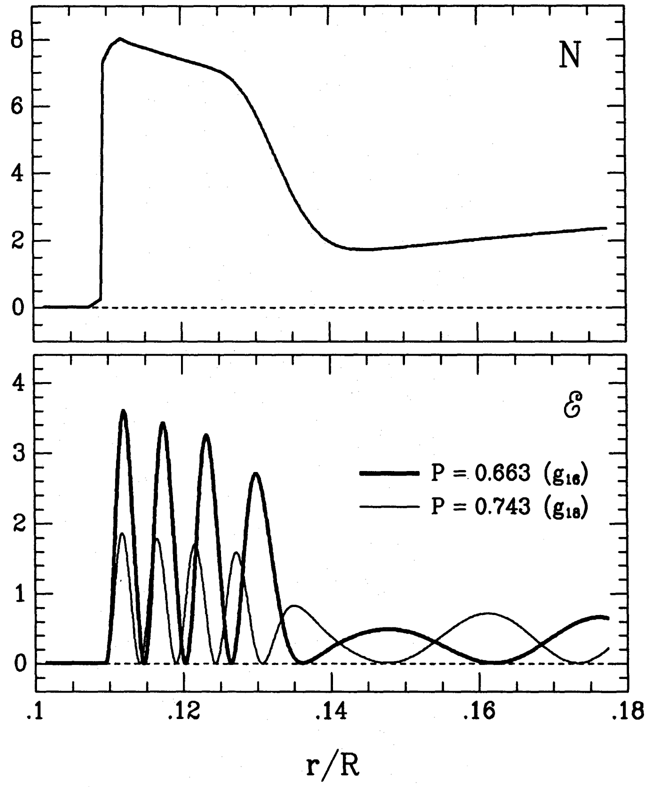

Figure 12. Top: Brunt–Väisälä frequency in the μ-gradient zone of the SPB model of Fig. 1. Bottom: kinetic energy density for modes g_{16} and g_{18} ($l=2$).

trapping cycle, i.e. the period difference between consecutive ΔP minima, undergoes large changes as the μ-gradient develops during the main-sequence evolution. The amplitude of ΔP deviations, on the other hand, should be rather sensitive to the steepness of the μ-gradient. Also, any effect of convective overshooting (if present) should have a strong bearing on the behaviour of ΔP.

The observational determination of ΔP might be a formidable task, however. The high-order g-mode spectra are complicated by the effect of rotational splitting. In fact, only in the most slowly rotating B-type objects, such as Waelkens's (1991) original SPB stars, does the concept of splitting apply. The requirement is that the angular velocity of rotation is sufficiently less than the oscillation frequency of the mode considered. This translates to $v_{\rm rot} \ll 2\pi R/P$. The model discussed in Section 4 has a radius of 3.13 $R_\odot$, and the longest unstable period is nearly 2 d. In this case, rotation may be regarded as a perturbation if $v_{\rm rot} \ll 80\ {\rm km\ s^{-1}}$.

In Fig. 13 we show the change in the distribution of the $l=1$ mode frequencies with an increase of $v_{\rm rot}$. The effects of rotation were calculated using the method developed by Dziembowski & Goode (1992), which is accurate to $O(\varepsilon^3)$ terms, where ε is the ratio of the rotational frequency to the oscillation frequency. The lines connecting mode frequencies display little curvature, which shows that the linear theory is still approximately valid in the range of rotational velocities considered. The plot shows how complicated mode identification in the SPB stars may be. The multiplets are already beginning to overlap at $v_{\rm rot} \approx 3\ {\rm km\ s^{-1}}$. Furthermore, near the intersection points, the beat periods are very long. Let us note that even with no rotation the beat period for the neighbouring modes is nP, i.e. up to 70 d in the present case.

7 CONCLUSIONS

The agreement between the positions of SPB stars and the theoretical instability domains in the HR and P versus $T_{\rm eff}$ diagrams makes us confident that we have correctly identi-

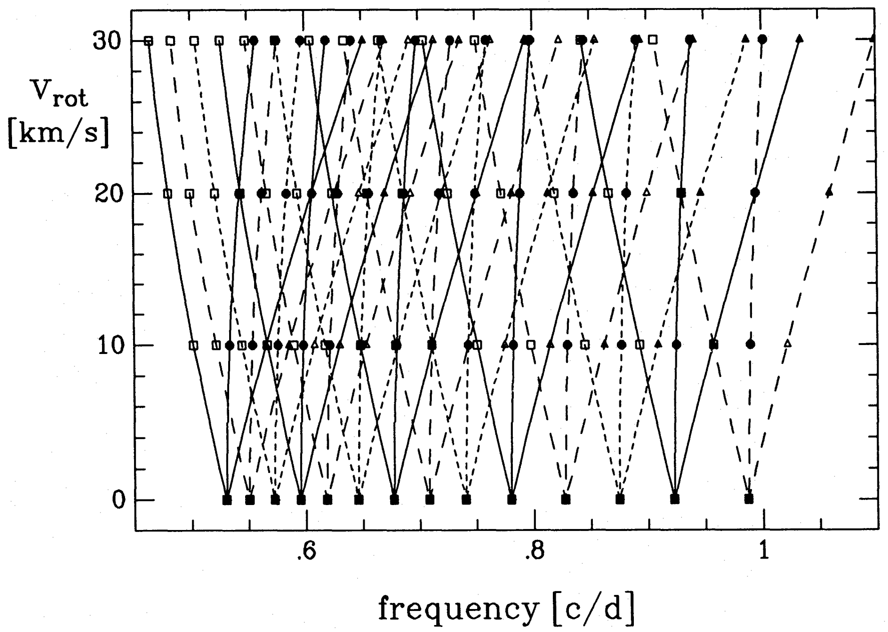

Figure 13. Rotational splitting for the $l=1$ modes in the SPB model of Fig. 1. The $m=-1$, $m=0$ and $m=1$ modes are marked by squares, circles and triangles, respectively.

fied the cause of pulsations observed in these objects. For a metallicity of $Z=0.02$, the SPB domain in the HR diagram, as determined by the instability of modes with $l \leq 2$, represents a low-luminosity extension of the β Cep domain. The driving mechanism is the same in both cases, but the unstable modes are different. While in the β Cep strip the low-order p-modes are unstable, in the SPB domain instability of high-order g-modes with periods ranging from 0.4 to 3.5 d occurs. The instability to the long-period modes continues into the β Cep strip, but only for high spherical harmonic degree l.

Prediction of the finite-amplitude development of this multimodal instability presents a challenge to the theory. We do not know the mechanism responsible for the amplitude limitation, and therefore we cannot predict which of the unstable modes may grow to an observable level. If only the high-l modes were to survive in the competition, no photometric variability could be seen. Instead, a contribution to the spectral line broadening should arise. There is an intriguing possibility that this may explain the excesses in the $v \sin i$ values observed in the main-sequence B-type stars (e.g. Fukuda 1982).

It has been suggested that the 53 Per-type stars might be related or even identical to the SPB variables (Waelkens & Rufener 1985). Our results support this conjecture. The coolest stars of this group, such as 53 Per itself and ι Her, fall into our theoretical domain of the low-l g-mode instability. 53 Per is indeed a photometric variable, and its periods agree well with the predictions of our models. For ι Her, radial velocity variations with a time-scale of about 1.5 d have been reported (Rogerson 1984) – this is also in a pertinent range. The higher temperature 53 Per-type stars fall above the low-l instability domain. The line profile variations observed in these stars might be understood in terms of pulsations in g-modes of *high* spherical harmonic degree l. As we have just pointed out, the instability of high-l modes extends well into the β Cep domain. Because these pulsations are probably multiperiodic, the correct determination of periods from the sparse spectroscopic data might be extremely difficult.

There is a possibility that the periodic variability seen in some Be stars (λ Eri-type behaviour) is also caused by the same opacity mechanism. Their spectral types and observed periods seem to suggest that this might be the case. We should stress, however, that in our stability survey we ignored the effects of rotation. This is justified only if the angular velocity of rotation is much less than the oscillation frequency. This condition is fulfilled in the SPB stars, but not in the λ Eri stars. An alternative mechanism of oscillation driving in these objects has already been proposed by Lee & Saio (1986). Their mechanism relies on the existence of the oscillatory convective modes in rapidly rotating cores. Rotational modulation due to surface inhomogeneity may also explain the variability if only one period is present. Balona (1992) favours these two proposals, and argues against metal opacity driving. His argument is based on the discovery of a large number of λ Eri stars and the simultaneous absence of β Cep stars in a metal-poor SMC cluster, NGC 330. We have pointed out, however, that at $Z=0.01$ a significant SPB instability domain still survives, while the β Cep domain is absent. Thus Balona's argument is not necessarily valid.

The discovery of g-mode oscillations in B-type stars provides a very interesting opportunity to test stellar evolution theory. The frequencies of oscillation probe very well the innermost part of the radiative interior – the region where the effects of the hypothetical convective overshooting would be most felt. Measurement of rotational splitting in oscillation spectra may give us a unique opportunity to determine the rotation rate in the deep interiors of stars. The angular momentum transport is the least understood aspect of stellar evolution. It is especially important to know the rotation rate in the μ-gradient region, because it is controversial whether this region acts as a barrier for angular momentum transport.

We are well aware that the SPB stars are not easy targets for asteroseismology. With their long periods, low amplitudes and complicated frequency spectra, these objects require patience and skill from observers. Nevertheless, we believe that seismology of these stars could be as rewarding as that of the pulsating white dwarfs, and we strongly encourage continuous observational effort.

ACKNOWLEDGMENTS

We gratefully acknowledge that the stellar evolution code used by us was, in its basic form, developed by Bohdan Paczyński, Maciej Kozłowski and Ryszard Sienkiewicz. Carlos Iglesias and Forrest Rogers sent us opacity data prior to publication in a directly usable form. We are grateful to all these people for their essential contribution. AAP thanks the American Astronomical Society for partial financial support during work on this project. This work was supported in part by National Committee for Scientific Research Grant No. 2-1185-91-01.

REFERENCES

Baade D., 1988, in Cayrel de Strobel G., Spite M., eds, Proc. IAU Symp. 132, The Impact of Very High S/N Spectroscopy on Stellar Physics. Kluwer, Dordrecht, p. 217
Balona L. A., 1984, MNRAS, 211, 973
Balona L. A., 1987, in Cox A. N., Sparks W. M., Starrfield S. G., eds, Lecture Notes in Physics Vol. 274, Stellar Pulsation. Springer-Verlag, Berlin, p. 83
Balona L. A., 1990, MNRAS, 245, 92
Balona L. A., 1991, in Baade D., ed., ESO Conf. Proc. 36, Rapid Variability of OB-Stars: Nature and Diagnostic Value. ESO, Garching, p. 249
Balona L. A., 1992, MNRAS, 256, 425
Balona L. A., Engelbrecht C. A., 1985, MNRAS, 214, 559
Balona L. A., Shobbrook R. R., 1984, MNRAS, 211, 375
Bradley P. A., Winget D. E., Wood M. A., 1993, ApJ, 406, 661
Brassard P., Fontaine G., Wesemael F., Hansen C. J., 1992, ApJS, 80, 369
Burki G., 1983, A&A, 121, 211
Degryse K., Noels A., Gabriel M., Waelkens C., Smeyers P., 1992, A&A, 263, 137
Dziembowski W., 1977a, Acta Astron., 27, 95
Dziembowski W., 1977b, Acta Astron., 27, 203
Dziembowski W., 1993, in Weiss W. W., Baglin A., eds, Proc. IAU Colloq. 137, Inside the Stars. ASP Conf. Ser. Vol. 40. Astron. Soc. Pac., San Francisco, p. 521
Dziembowski W., Goode P. R., 1992, ApJ, 394, 670
Dziembowski W., Pamyatnykh A. A., 1993, MNRAS, 262, 204 (Paper I)
Floquet M., Hubert A. M., Janot-Pacheco E., Mekkas A., Hubert H., Leister N. V., 1992, A&A, 264, 177
Fukuda I., 1982, PASP, 94, 271
Grenon M., 1993, in Weiss W. W., Baglin A., eds, Proc. IAU Colloq. 137, Inside the Stars, ASP Conf. Ser. Vol. 40. Astron. Soc. Pac., San Francisco, p. 693
Grillo F., Sciortino S., Micela G., Vaiana G. S., Harnden F. R. J., 1992, ApJS, 81, 795
Hauck B., Mermilliod M., 1990, A&AS, 86, 107
Heynderickx D., 1991, PhD thesis, Katholieke Universiteit Leuven
Iglesias C. A., Rogers F. J., Wilson B. G., 1992, ApJ, 397, 717
Jerzykiewicz M., Sterken C., 1992, A&A, 261, 477
Kawaler S. D., 1990, in Cacciari C., Clementini G., eds, ASP Conf. Ser. Vol. 11, Confrontation between Stellar Pulsation and Evolution. Astron. Soc. Pac., San Francisco, p. 494
Le Contel J. M., Chapellier E., Le Contel D., Rau G., Endignoux A., Valtier J. C., Mevellon M., 1989, Acta Astron., 39, 227
Lee U., Saio H., 1986, MNRAS, 221, 365
McNamara B. J., 1985, ApJ, 289, 213
McNamara B. J., 1987a, ApJ, 312, 778
McNamara B. J., 1987b, in Cox A. N., Sparks W. M., Starrfield S. G., eds, Lecture Notes in Physics Vol. 274, Stellar Pulsation. Springer Verlag, Berlin, p. 92
Manfroid J., Renson P., 1989, A&A, 223, 187
Moskalik P., Dziembowski W., 1992, A&A, 256, L5
North P., Nicolet B., 1990, A&A, 228, 78
Rogerson J. B., 1984, AJ, 89, 1876
Rufener F., 1988, Catalogue of Stars Measured in the Geneva Observatory Photometric System, 4th edn. Observatoire de Genève, Sauverny
Slettebak A., 1988, PASP, 100, 770
Smith M. A., 1977, ApJ, 215, 574
Smith M. A., Karp A. H., 1976, in Cox A. N., Deupree R. G., eds, Proc. Solar and Stellar Pulsation Conf., Los Alamos, p. 289
Smith M. A., Fitch W. S., Africano J. L., Goodrich B. D., Halbedel W., Palmer L. H., Henry G. W., 1984, ApJ, 282, 226
Stellingwerf R. F., 1978, ApJ, 227, 935
Struve O., 1955, Sky Telesc., 14, 461
Tassoul M., 1980, ApJS, 43, 469
van Genderen A. M. et al., 1992, A&A, 259, 574
Waelkens C., 1987, in Cox A. N., Sparks W. M., Starrfield S. G., eds, Lecture Notes in Physics Vol. 274, Stellar Pulsation. Springer Verlag, Berlin, p. 75
Waelkens C., 1991, A&A, 246, 453
Waelkens C., Heynderickx D., 1989, A&A, 208, 129
Waelkens C., Rufener F., 1985, A&A, 152, 6
Winget D. E., van Horn H. M., Hansen C. J., 1981, ApJ, 245, L33
Winget D. E. et al., 1991, ApJ, 378, 326